

Relative Orientation between the  $\beta$ -Ionone Ring and the Polyene Chain for the Chromophore of Rhodopsin in Native Membranes<sup>†</sup>Paul J. R. Spooner,<sup>\*,‡</sup> Jonathan M. Sharples,<sup>‡</sup> Michiel A. Verhoeven,<sup>§</sup> Johan Lugtenburg,<sup>§</sup> Clemens Glaubitz,<sup>‡,||</sup> and Anthony Watts<sup>\*,‡</sup>

The Biomembrane Structure Unit, Department of Biochemistry, University of Oxford, South Parks Road, Oxford OX1 3QU, United Kingdom, and Leiden Institute of Chemistry, Gorlaeus Laboratories, Einsteinweg 55, 2333 CC Leiden, The Netherlands

Received January 7, 2002; Revised Manuscript Received April 4, 2002

**ABSTRACT:** Rotational resonance solid state nuclear magnetic resonance has been used to determine the relative orientation of the  $\beta$ -ionone ring and the polyene chain of the chromophore 11-Z-retinylidene of rhodopsin in rod outer segment membranes from bovine retina. The bleached protein was regenerated with either 11-Z-[8,18-<sup>13</sup>C<sub>2</sub>]retinal or 11-Z-[8,16/17<sup>13</sup>C<sub>2</sub>]retinal, the latter having only one <sup>13</sup>C label at either of the chemically equivalent positions 16 and 17. Observation of <sup>13</sup>C selectively enriched in the ring methyl groups, C16/17, revealed alternative conformational states for the ring. Minor spectral components comprised around 26% of the chromophore. The major conformation (~74%) has the chemical shift resolution required for measuring internuclear distances to <sup>13</sup>C in the retinal chain (C8) separately from each of these methyl groups. The resulting distance constraints, C8 to C16 and C17 (4.05 ± 0.25 Å) and from C8 to C18 (2.95 ± 0.15 Å), show that the major portion of retinylidene in rhodopsin has a twisted 6-*s-cis* conformation. The more precise distance measurement made here between C8 and C18 (2.95 Å) predicts that the chain is twisted out-of-plane with respect to the ring by a modest amount (C5–C6–C7–C8 torsion angle = -28 ± 7°).

The cascade of biochemical events leading to the visual response process is triggered by the photoisomerization of the chromophore, 11-Z-retinylidene, within the G-protein-coupled receptor, rhodopsin (*I*). Solid state nuclear magnetic resonance (NMR) has provided precise conformational details for the central segment of the polyene chain that undergoes photoisomerization in <sup>13</sup>C-labeled retinals introduced into bovine rhodopsin (2, 3). The  $\beta$ -ionone ring in retinylidene has been assumed to adopt a *cis* conformation between unsaturation within the ring (C5–C6 bond) and in the adjoining portion of the polyene chain (C7–C8 bond), based mainly on comparisons of <sup>13</sup>C NMR chemical shift information with that of model compounds (4). This 6-*s-cis* conformation is also fitted to the electron density assigned to this portion of the chromophore, within a recent crystal structure of bovine rhodopsin at 2.8 Å resolution (5). Although 6-*s-cis*-retinal and related compounds are nonplanar (6), the torsion angle between the polyene chain and the ring

within the protein has not been determined directly. How this geometry influences the electronic distribution in the chromophore and its consequent role in the characteristic “opsin shift” in light absorption on binding with the protein therefore remains uncertain. Furthermore, deuterium NMR measurements conducted in this laboratory on the orientation of the retinylidene methyl groups in bovine rhodopsin, reconstituted into bilayers of a saturated lipid, fitted best to a twisted 6-*s-trans* conformation (7). A further study (8) has predicted that the 6-*s-trans* conformer represents the minimum energy state of the chromophore and argues that this, combined with the NMR evidence, calls into question the structure derived from X-ray crystallography. In view of these contrasting arguments, the conformation around the ring segment of the chromophore in the dark-adapted protein is specifically addressed here using solid state NMR methods that are particularly well-suited for this purpose.

In what was the first application of solid state NMR for obtaining specific structural information on a membrane protein, the rotational resonance method was used to measure internuclear distances between isolated <sup>13</sup>C spin pairs in the retinylidene chromophore of the light-activated proton pump, bR<sup>1</sup> (9). This work confirmed previous predictions that the chromophore adopts a 6-*s-trans* conformation in this protein. The planar 6-*s-trans* conformation in bR could be distinguished from the alternative 6-*s-cis* case by a single

<sup>†</sup> This work was supported by grants to A.W. from BBSRC for Professorial Fellowship (for A.W. on Grant no. 43/SF09211), a Senior Research Associate (for P.J.R.S. on Grant no. 43/014769), a “priority area” graduate studentship (J.S.), from BBSRC and from MRC (U.K.) (Grant no. G9901287). C.G. is the recipient of a DFG Emmy Noether Research Fellowship. The Biomembrane Structure Unit was established with JREI grants from HEFCE/BBSRC (JROXWA).

<sup>\*</sup> To whom correspondence should be addressed. (P. S.) Tel.: +44-018650 275270. Fax: +44-01865 275234. E-mail: spooner@bioch.ox.ac.uk. (A. W.) Tel.: +44-01865 275268. Fax: +44-01865 275234. E-mail: awatts@bioch.ox.ac.uk.

<sup>‡</sup> University of Oxford.

<sup>§</sup> Gorlaeus Laboratories.

<sup>||</sup> Current address: FMP Berlin, Robert Rössle Strasse 10, 13125 Berlin, Germany.

<sup>1</sup> Abbreviations: bR, bacteriorhodopsin; MAS, magic-angle spinning; CP, cross polarization; *T*<sub>2</sub>, spin–spin relaxation time; *T*<sub>2</sub><sup>zq</sup>, zero-quantum spin–spin relaxation time;  $\omega_r$ , MAS rotation speed;  $\Delta\omega_{iso}$ , isotropic chemical shift difference; MAOSS, magic-angle-oriented sample spinning.

measurement between a  $^{13}\text{C}$  located in the chain and a  $^{13}\text{C}$  in the ring. Distinguishing between alternate nonplanar conformations for retinylidene in rhodopsin will only be possible from multiple distance measurements. Here, rotational resonance measurements are conducted between  $^{13}\text{C}$  in the chain of retinylidene in rhodopsin and each of three individual methyl locations in the ring, in an effort to determine not only the absolute conformation in this segment of the chromophore but also the torsion angle between the ring and the polyene chain.

## EXPERIMENTAL PROCEDURES

**Sample Preparation.** The synthesis and purification of 11-Z-[8,18- $^{13}\text{C}_2$ ]retinal and 11-Z-[8,16/17- $^{13}\text{C}_2$ ]retinal were as described previously (10). All manipulations involving rhodopsin regenerated with  $^{13}\text{C}$ -labeled retinals were conducted in dim red light and under an atmosphere of argon. Rod outer segment membranes were isolated from fresh bovine retina (11) and bleached using a white light source (250 W) for removal of the native retinal in its all *trans* state (12). The rhodopsin in these membranes was then regenerated (12) at a 1:1 molar ratio with either 11-Z-[8,18- $^{13}\text{C}_2$ ]retinal (260 nmol) or 11-Z-[8,16/17- $^{13}\text{C}_2$ ]retinal (500 nmol), and the membranes were washed using 50 mM  $\beta$ -cyclodextrin to remove nonincorporated material (13), yielding 7.3 and 12 mg, respectively, of labeled rhodopsins. During the synthesis of 11-Z-[8,16/17- $^{13}\text{C}_2$ ]retinal, either carbon 16 or carbon 17 is enriched to 99% with  $^{13}\text{C}$ . Because these products are chemically equivalent and cannot be separated, rhodopsin regenerated with these retinals contains retinylidene labeled at either C8 and C16 or C8 and C17 in equal proportions. Two further membrane samples were regenerated under identical conditions with nonlabeled 11-Z-retinal (gift from A. Albert, Storrs, Connecticut) at the amounts equal to those used for the regenerations with labeled retinals. The washings with cyclodextrin solution also removed a portion of the rod outer segment membrane lipid, although the remaining lipid is sufficient to fully solvate the protein in these membranes (>30 lipids per protein; W. de Grip, personal communication). On the basis of the  $A_{280}/A_{500}$  from solubilized membranes (13), >90% of the bleached protein was regenerated back to rhodopsin using the molar equivalent amounts of retinals and their  $A_{365}/A_{500}$  (13) showed that <5% of labeled material was not properly incorporated into the protein.

**NMR Methods.** The entire amounts of each rhodopsin sample, regenerated with  $^{13}\text{C}_2$ -labeled or unlabeled retinal, were packed into 4 mm diameter sample rotors for a Chemagnetics (Varian) Apex MAS NMR probe and rotated briefly at moderate speed. Samples were then snap-frozen by immersing the MAS rotors in liquid nitrogen and then subsequently kept frozen at  $-60^\circ\text{C}$  during the MAS NMR measurements or at  $-80^\circ\text{C}$  for storage. All NMR measurements were conducted at 125.8 MHz for  $^{13}\text{C}$  (500.1 MHz for protons) using a Chemagnetics (Varian) Infinity spectrometer. The rotational resonance experiment for homonuclear recoupling and rotary-driven exchange of magnetization between the isolated  $^{13}\text{C}$  spin pairs was as originally described (14), except that the initial carbon magnetization was created by CP using a 30% linear ramp (15) on the output for the carbon frequency and also that the selective inversion of one of the enriched  $^{13}\text{C}$  spins was accomplished

with DANTE pulses. Proton field strengths of 63 kHz used for the CP were increased to 100 kHz for decoupling during the rotational resonance mixing (exchange) period and during signal acquisition, while field strengths used for  $^{13}\text{C}$  were around 63 kHz throughout. Rotational resonance exchange curves were fitted to the experimental data using RR FIT (16), a modification of the CC2 software (Malcolm Levitt, Southampton) derived from the original theoretical treatment (17). This parameter fitting procedure calls error minimization routines that are part of the MINUIT package (CERN Program Library).

$T_2$  was measured with the Hahn-spin echo, and relaxation rates were combined for the spin pairs to provide an estimate of  $T_2^{\text{eff}}$  required in the analysis of rotational resonance exchange data. Proton  $T_1$  measurements were made from inversion–recovery of proton magnetization followed by CP for indirect detection on the labeled  $^{13}\text{C}$  spins.

Tensor values used in the simulations (chemical shift anisotropy, asymmetry parameter) were determined for labeled retinylidene sites in the rhodopsin samples from the analysis of rotational sidebands in spectra recorded at  $-60^\circ\text{C}$  with slow sample spinning (2.5 kHz) using the Herzfeld–Berger method (18) applied by an interactive routine (19) with the SPEEDYFIT program. All rotational resonance was conducted at the  $n = 1$  condition ( $\omega_r = \Delta\omega_{\text{iso}}$ ) where simulations were shown to be insensitive to the absolute and relative orientations of the chemical shift tensors, as expected from theoretical considerations (17).

## RESULTS AND DISCUSSION

**Spectral Characteristics of  $^{13}\text{C}$ -Labeled Chromophore in Rhodopsin.** CP MAS  $^{13}\text{C}$  spectra from the membranes regenerated with the labeled retinals are shown in Figure 1. The alkyl regions in these spectra have been prepared with the DANTE inversion for observation of Zeeman exchange. The upper spectrum in each case comprises of signals from the selectively enriched chromophore combined with the natural abundance  $^{13}\text{C}$  contribution from the membranes. Using measurements recorded under identical conditions for the rhodopsin regenerated with nonlabeled retinal, it was possible to subtract out effectively the natural abundance  $^{13}\text{C}$  background contribution from the membranes and reveal the NMR signals solely from the enriched sites in the retinylidene (Figure 1A,B, lower spectra). The resonance from the C8 position in the polyene chain in both samples appears at 139.4 ppm whereas the C18 ring methyl is located at 22.1 ppm and C16 and C17 intensity appears resolved in the protein environment at 30.8 and 26.4 ppm (labeled *a* and *b*, respectively), in contrast to free retinal where these sites are equivalent and appear at an intermediate chemical shift (28.8 ppm measured in heptane, ref 12).

The difference in peak heights between spectral components *a* and *b*, inverted in Figure 1B (lower spectrum), is not consistent with the equal distribution of label between C16 and C17 in the retinal used to regenerate the protein.  $T_1$  values for the protons providing polarization for these methyl carbons were relatively short ( $\sim 0.75$  s) and not sufficiently different (within 0.15 s) to account for the differences between resonances *a* and *b*. To quantify properly

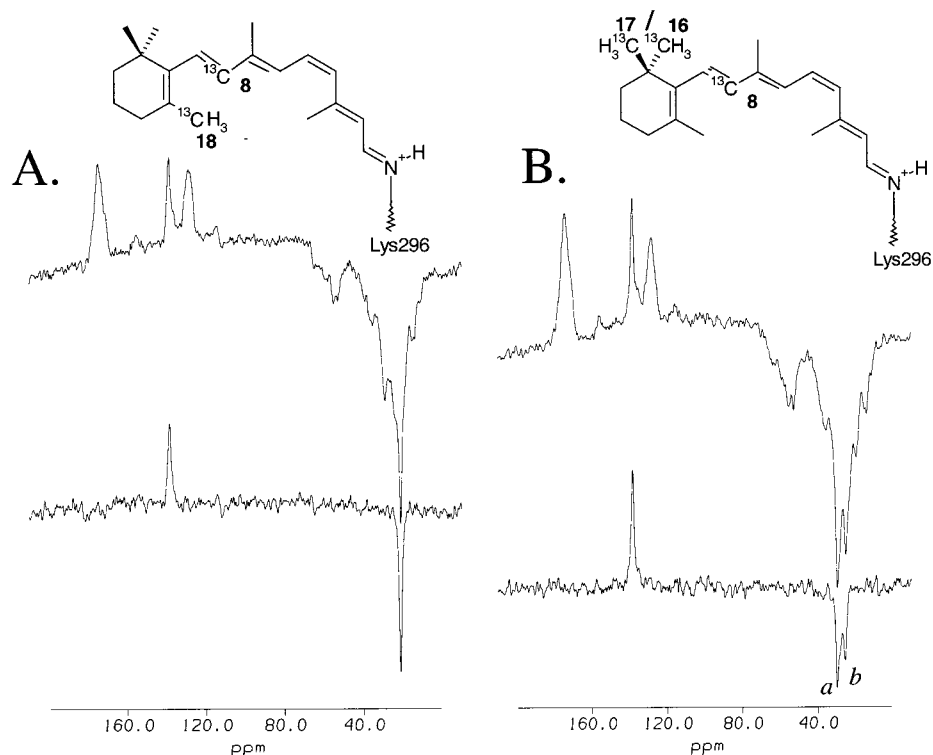


FIGURE 1:  $^{13}\text{C}$  CP MAS spectra from bovine rod outer segment membranes containing rhodopsin regenerated with 11-Z-retinal selectively labeled with  $^{13}\text{C}$  spin pairs at positions C8 and C18 (A) or C8 with C16 or C17 in equal proportions (B) as indicated in the respective insets. Spectra with selective inversion of the methyl region for observation of rotational resonance exchange from the membranes and labeled chromophore (upper spectra) and following subtraction of the natural abundance contribution from the membranes to leave signals only from the sites of labeling in the retinylidene chromophore (lower spectra).

the intensities in this spectral region, a ramped CP MAS NMR spectrum was recorded under equilibrium conditions (4 s recycle time) from the labeled and nonlabeled samples. When no line broadening was introduced in the data processing, the background-subtracted spectrum (Figure 2A) revealed additional spectral components appearing at intermediate chemical shifts and merging with resonance *a*. Two additional spectral components (*c* and *d* in Figure 2A) were deconvoluted from this region, together accounting for 26% of the total intensity from the labeled methyl groups. After the minor component (*c* + *d*) was removed from the spectral simulation (Figure 2B), the line width of resonance *a* was 110 Hz and accounted for 40% of the total intensity and the remaining 34% of the intensity resided in resonance *b* with a larger line width of 155 Hz. These intensities for resonances *a* and *b* (Figure 2B) were sufficiently similar for them to be assumed to represent the two labeled methyl groups (C16 and C17) that exist within the major structural form (comprising 74%) of retinylidene in the protein, and they are well-resolved for their individual, selective recoupling with C8 by rotational resonance. The separation from the minor resonances exceeded 150 Hz, which is beyond the line width of the closer major resonance *a* (30.8 ppm). The resolution observed here for the minor component is also degraded by field drift occurring during the length of time required for the equilibrium measurement (~22 h), and so, their separation from the major resonances will be improved over the shorter incremental times required to record rotational resonance exchange (~3 h). Taking all these factors into consideration, overlap with the minor component is expected to introduce only a small error in the exchange measured with C8 in these experiments. Indeed, the minor

component appears to be unaffected while resonance *a* is depleted by selective exchange with C8 (Figure 2C).

**Rotational Resonance Recoupling.** Rotational resonance exchange between C8 and each of the two major C16/C17 signals is represented in Figure 3A as a function of time. The net magnetization ( $\langle I_z - S_z \rangle$ ) following inversion of the methyl signal ( $S_z$ ) has been corrected for the proportion of C8 label participating in rotary resonant exchange with the individual methyl resonances and normalized to the initial corrected net magnetization averaged from a number of short (<0.1 ms) mixing times. The exchange rates measured with the C16 and C17 are indistinguishable from each other in these experiments. Despite the differences in line width noted above between the major resonances *a* and *b* from C16 and C17 (Figure 2A,B), these signals had similar spin-spin relaxation rates, providing an estimate of  $T_2^{ZQ}$  of 6 ms ( $\pm 1$  ms) for the coupling of each to C8. The additional broadening in component *b* was therefore not caused by enhanced transverse relaxation but may be explained by small variations in the C16/C17 methyl group orientations, based on the structural interpretation given below for the chemical shift inequivalence observed between these groups within the protein. The similarity in rates of rotational resonance exchange and in  $T_2^{ZQ}$  processes meant that the dipolar couplings with C16 and C17 from C8 could not be distinguished in these experiments and the exchange data for these were combined for the analysis. The best single parameter fit for the dipolar coupling between C8 and both methyl groups corresponds to an internuclear distance of 4.05 Å (solid curve in Figure 3A). The exchange curves simulated for the internuclear distances of 3.80 and 4.30 Å encompass most of the variability shown in the data (Figure 3A) that

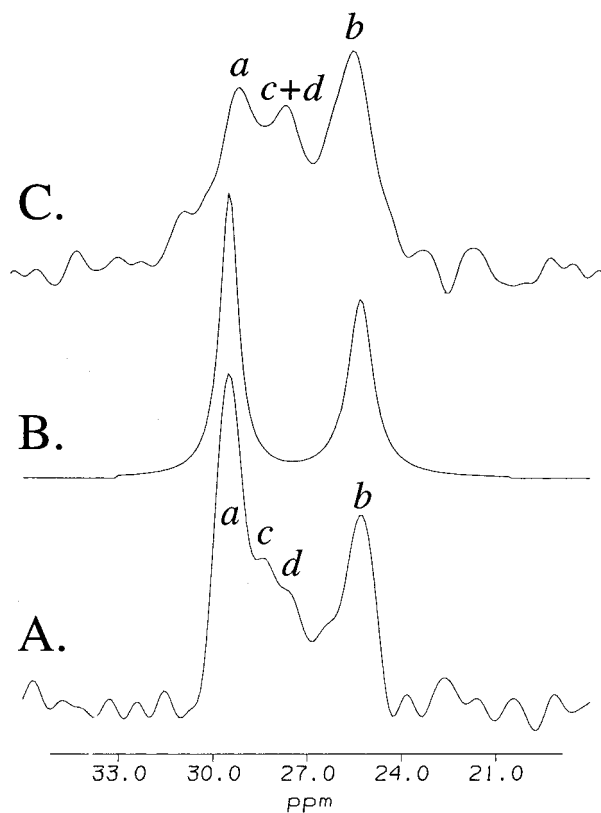


FIGURE 2:  $^{13}\text{C}$  CP MAS spectrum (background subtracted; see text) of retinylidene C16 and C17 in rhodopsin recorded to show equilibrium intensities (recycle time = 4 s; 20 000 acquisitions processed without line broadening) and minor components between the major low-frequency (26.4 ppm) and high-frequency (30.7 ppm) resonances (A). Spectral simulation of C16 and C17 resonances in the major (~74%) retinylidene component with intensity from minor components subtracted out (B). Spectrum of C16/17 signals (background subtracted; see text) with the high-frequency resonance depleted by 10 ms of  $n = 1$  rotational resonance exchange with C8 showing that the minor components merge as a single resonance from 6000 acquisitions processed with 70 Hz line broadening (C).

arises from nonsystematic errors in the measurements. These include spectrometer instabilities and errors from spectral subtraction and integration. The accuracy of the measurement will be affected by certain systematic errors, mainly arising from the estimate of  $T_2^{\text{eff}}$  and from estimating the proportion of minor forms. The latter error is not expected to exceed the 6% difference found between the intensities from C16 and C17 in the major form of retinylidene. Errors in the measured tensor values and their orientations are not a significant factor in the analysis here. No significant decay in net magnetization was observed over these experimental mixing times at 1 kHz away from  $n = 1$  rotational resonance (Figure 3A).

The exchange behavior between the C8 and the C18 methyl group in rhodopsin (Figure 3B) is strikingly different from that with the C16/17 methyl groups. The experimental data obtained from these measurements (Figure 3B, open circles) describe a biphasic exchange in which the majority of net magnetization exchanges rapidly (<5 ms), and this is followed by a very slow decrease over the longer mixing times (to 30 ms). Rotational resonance exchange can often be observed to "tail off" at longer mixing times due to various experimental limitations such as unstable spinning, large spectral line widths, and imperfect proton decoupling.

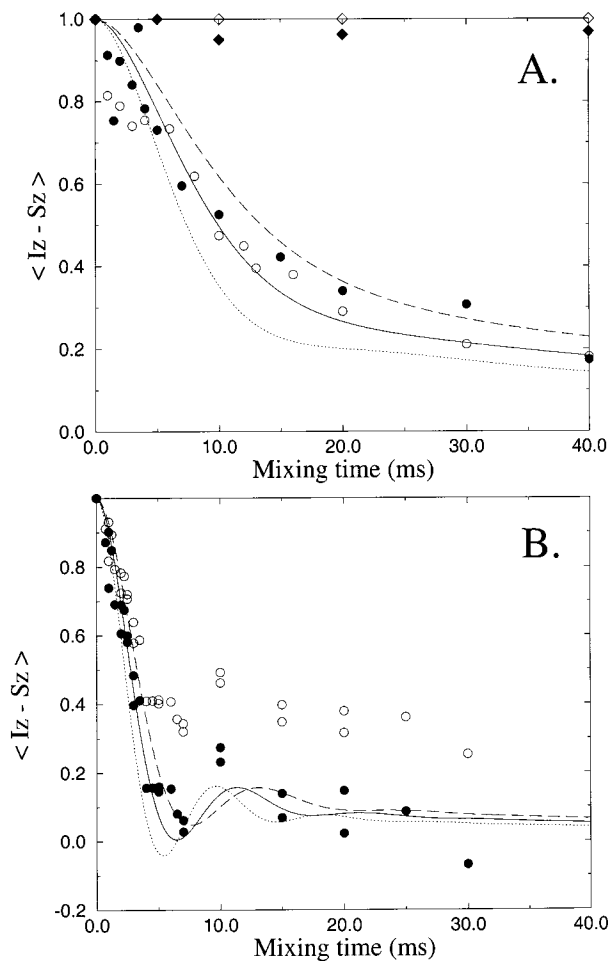


FIGURE 3: Exchange data under  $n = 1$  rotational resonance between the retinylidene  $^{13}\text{C}$  spin pairs in bovine rhodopsin showing net magnetization as a function of the rotational resonance mixing time. Exchange between C8 and the C16/C17 for the high-frequency (open circles) and low-frequency (closed circles) methyl resonances and at 1 kHz away from  $n = 1$  rotational resonance for the high-frequency (open diamond) and low-frequency (closed diamond) methyl resonances (A). Net magnetization was corrected for the fraction of C8 participating in rotational resonance in each case (as specified in text), and the curves are from the simulations corresponding to a best-fitting internuclear distance of 4.05 Å (solid line) and for 4.30 (dashed line) and 3.80 Å (dotted line) representing an estimation of the upper and lower limit. Experimental data for magnetization exchange are between C8 and C18 (open circles), and data are corrected to represent the rapid phase of exchange (closed circles) for the major component. Simulated curves are for the best fit to the internuclear distance of 2.95 Å (solid curve) and for the estimated upper and lower limits of 3.10 (dashed line) and 2.80 Å (dotted line), respectively (B).

However, the high spinning stability maintained in experiments here ( $\pm 3$  Hz), the acceptable line widths ( $\sim 100$ – $150$  Hz), and the ability to sustain rapid rotational resonance in model systems with strong homo- and heteronuclear couplings (e.g., 1,2- $^{13}\text{C}$ glycine) indicate that the experimental setup was not particularly susceptible to these limitations. Furthermore, the slow phase of exchange occurs at a sharp discontinuity and does not appear to damp out the oscillation in the rapid exchange process, occurring later at around 10 ms exchange time, further suggesting that the effect arises from an independent exchange process. It is possible, therefore, that the slow exchange is occurring within the minor form, as detected from observation of the C16- and C17-labeled sites, but is not being resolved in the spectra

Table 1: Summary of  $^{13}\text{C}$  Chemical Shift and Distance Measurements for Retinal in Rhodopsin, Including Data Reported for bR and Crystalline Analogues

	chemical shifts (ppm)		
	C8	C16/17	C18
bovine rhodopsin (native membrane)	139.4 <sup>a</sup>	30.7/26.4 <sup>a</sup>	22.1 <sup>a</sup>
6- <i>s-cis</i>			
all <i>trans</i> retinal	138.2 <sup>b</sup>	31.7/28.9 <sup>c</sup>	23.3 <sup>c</sup>
retinoic acid	138.9 <sup>b</sup>	32.5/28.7 <sup>d</sup>	24.1 <sup>d</sup>
bR (purple membrane)	131.6, 132.7 <sup>b</sup>	28.9 <sup>b</sup>	22.0 <sup>b</sup>
6- <i>s-trans</i>			
13- <i>cis</i> -retinal	<133 <sup>b</sup>		
retinoic acid	130.9 <sup>d</sup>	30.9/27.3 <sup>d</sup>	20.8 <sup>d</sup>
	distance from C8 (Å)		
	C16/17	C18	
bovine rhodopsin	4.05 ± 0.25 <sup>a</sup>	2.95 ± 0.15 <sup>a</sup>	
bR		~4.1 <sup>e</sup>	

<sup>a</sup> Measured here and referenced against adamantane methylene (38.6 ppm). <sup>b</sup> Ref 29. <sup>c</sup> Protonated Schiff base form: ref 30. <sup>d</sup> Ref 30. <sup>e</sup> Ref 9.

from C8 or C18 in the protein chromophore; all structural forms are simultaneously recoupled during rotational resonance.

To obtain a good fit to the intensity remaining at longer mixing times, a correction of 30% was applied for the proportion of C8 and C18 not participating in the major rapid phase (<5 ms) of exchange. Rounding up the proportion of nonexchanging minor components by a few percent over that which was deconvoluted from the equilibrium spectrum of C16 and C17 (26%) is also justified from the 6% difference in intensities between the methyl signals in the major component. This indicated that a small proportion of the minor component intensity was not successfully deconvoluted from resonance *a* in the equilibrium spectrum. The best fit to the corrected data for the exchange between C8 and C18 (filled circles, Figure 3B) corresponds to an internuclear distance of 2.95 Å (Figure 3B). The rapid exchange, relatively small experimental scatter in the exchange data, and distinctive oscillatory features combine to provide a relatively narrow range of uncertainty in this measurement, estimated from the variability in the data to be between 2.80 and 3.10 Å (Figure 3B). This range again does not account for any of the possible systematic errors mentioned above. The assumption implicit in the analysis that the minor, slow phase of magnetization exchange will not significantly contribute to the rapid exchange rate for the major population of retinylidene in rhodopsin (~70%) is reasonable over the short times (~5 ms) required for the majority of this exchange to be completed.

A summary of the isotropic chemical shift and structural data derived from this study is given in Table 1 together with data from other sources on related compounds. While the ring methyl chemical shifts are not very informative about the absolute conformation of the ring to the chain, the C8 chemical shift is highly sensitive to the isomeric state around the C6–C7 bond. The C8 chemical shift decreases by as much as 8 ppm on changing from 6-*s-cis* to 6-*s-trans*, possibly due to a steric effect with the C16/C17 methyls. The retinal C8 chemical shift in rhodopsin is similar to that

previously reported (139.2 ppm; ref 4) and is well within the range of chemical shift for the 6-*s-cis* forms, as also noted previously (4), in contrast to retinal in bR, which exhibits a 6-*s-trans* shift at C8. The mean distance between the C8 and the C16/C17 methyl groups in rhodopsin is equivalent to that used to simulate rotational resonance exchange between C8 and C18 in bR, indicating that the major form of retinylidene has the opposite conformation about the C6–C7 bond in these two proteins. Comparing the distances from C8 to C18 (2.95 Å) and to C16 and C17 (4.05 Å) also describes the 6-*s-cis* orientation for the major portion of the chromophore in rhodopsin. The minor form of the chromophore, if responsible for the slow phase of exchange between C8 and C18, should tend toward the opposite 6-*s-trans* conformation of the ring. This interpretation is reinforced by the finding that both the additional minor resonances observed from C16 and C17 appear to exchange more rapidly with C8 than the major resonances (data not shown), which is also consistent with the alternate, 6-*s-trans* conformation. However, the absence of any discrete portion of the C8 signal appearing at lower chemical shift, as noted above for the 6-*s-trans* analogues, may indicate that the minor form did not adopt a well-defined planar state. The minor component would also appear to be present in roughly equal proportions in both regenerated protein samples (26–30%). The lack of further labeled retinals prevented any investigation of whether these levels of minor component could be affected by adaptations in the regeneration procedure.

The chemical shift inequivalence between the C16 and the C17 methyl groups can be accounted for solely on the basis of intramolecular steric effects within the chromophore. Indeed, chemical shift inequivalence between these methyl groups is observed in the crystalline analogues (Table 1) and this more clearly relates to differences in the intramolecular interactions for these groups. The inequivalence between C16 and C17 in rhodopsin is larger than in the crystalline analogues reported here (Table 1) and involves greater shielding for one of these methyl groups (lowest chemical shift). However, the 4.3 ppm separation observed here between the C16 and the C17 signal in the protein is well within the range of chemical shift differences found between methyl groups in equatorial and axial orientation on cyclohexanes (20, 21). Specifically, where an axial methyl is buttressed with a geminal equatorial methyl, as possible between C16 and C17, then its steric interaction with the axial protons on the  $\gamma$ -carbons in a cyclohexane ring can result in a shift of 4.2 ppm per ring proton interaction (22). This matches the shift difference observed here where the C16 or C17 methyl group can interact with an axial ring proton from only one  $\gamma$ -carbon (C3) in the retinylidene ring. Although this agreement shows that an equatorial and axial configuration for C16 and C17 can fully account for their differences in chemical shift observed within the protein, it does not yield the precise orientations of these methyl groups on the ring. Without such specific structural information, the distance constraints from the C16 and C17 methyl groups cannot be used to predict the degree of twist in the polyene chain with any great certainty. Thus, an estimation of the twist between the polyene chain and the ring currently relies only on the distance measured between the C8 and the C18 methyl group. This shorter internuclear distance is nonethe-

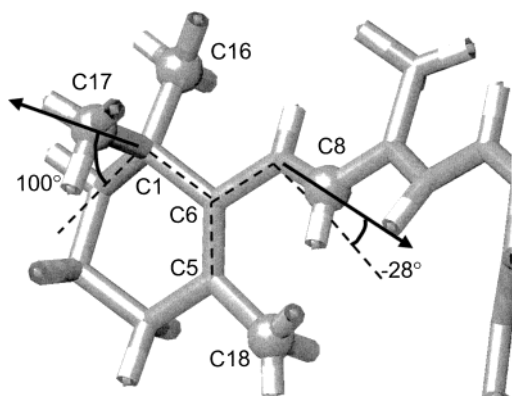


FIGURE 4: Orientational manipulation of the 11-Z-retinal structure from crystal data (23) obtained by incorporating the internuclear distance measurements (Table 1) made here. The C8–C18 internuclear distance of 2.95 Å is used here to predict the out-of-plane twist in the retinal chain (C5–C6–C7–C8 torsion angle =  $-28^\circ$ ). The orientation selected for the axial and equatorial configuration of C17 and C16, respectively, places the methyl groups equidistant from C8 at 4.19 Å (measured  $4.05 \pm 0.25$  Å for both groups).

less obtained with greatest precision, and this measurement is made from the most rigid segment of the ring (C4–C5–C6), which is least likely to be perturbed in the protein.

Starting from the crystal structure of 11-Z-retinal (23), as used for modeling the chromophore from other NMR studies (3) and also in the protein crystal data (5), the distance measured between C8 and C18 (2.95 Å) predicts an out-of-plane twist of  $28^\circ$  in the chain as shown in Figure 4. The structure presented in Figure 4 also has the C16 and C17 methyl groups equidistant (4.19 Å) from C8. This was achieved by tilting the C2–C1–C6 ring segment to bring C17 more into axial orientation, as required by the larger steric shift observed for C16 or C17 in the protein, as compared with 6-*s-cis* crystalline analogues (Table 1). This reorientation within the ring increases the C5–C6–C1–C17 torsion angle to  $+100^\circ$ , only  $5^\circ$  more toward the axial orientation than in the crystalline retinal and so involves far less manipulation of the starting structure than would be necessary for bringing the C16 methyl into axial orientation. The twist in the chain is made in the opposite sense to the C17 reorientation (C5–C6–C7–C8 torsion angle =  $-28 \pm 7^\circ$ ), since this provides the largest twist while maintaining C16 and C17 equidistant from C8 and agrees with the sense of twist used to fit the retinylidene electron density resolved from the current crystallographic data on the dark-adapted protein (5). The out-of-plane twist is important for reducing steric interactions between the chain and the ring, thereby stabilizing retinylidene in the ground state, dark-adapted rhodopsin. The  $28 \pm 7^\circ$  twist arrived at here from the shorter C8–C18 measured internuclear distance is, however, quite modest as compared with that generally found in the naturally occurring 6-*s-cis* carotenoid analogues, which normally range between 30 and  $70^\circ$  (6). The  $\pm 7^\circ$  range on this torsion angle is strictly only obtained from the upper limit for the C8–C18 distance (3.1 Å), the lower distance limit (2.8 Å) being too short to be attained by simply manipulating this torsion angle in the starting structure. This limitation emphasizes the need to incorporate distances to all ring methyl groups in order to specify full limits on the torsion angle as well as improving the overall certainty in its estimation. Combining all distances measured

here will require a specific determination of the C16 and C17 methyl group orientations with respect to the ring.

The current results show decisively that the ring in the rhodopsin chromophore has a preferred 6-*s-cis* orientation in the dark-adapted protein, in contrast to the twisted 6-*s-trans* conformation deduced for the  $^2\text{H}$  NMR static and MAOSS measurements (7). A number of studies have shown that a variety of retinal analogues can be accommodated within the binding pocket in rhodopsin (24–26), which may help explain the existence of minor alternative structural forms in the current study. It was possible that a similar degree of structural heterogeneity with the chromophore could have interfered with the analysis of methyl orientations from the  $^2\text{H}$  NMR measurements. Because the total  $^2\text{H}$  isotropic chemical shift dispersion is relatively small (ca. 10 ppm), different populations would cause a number of overlapping sideband families that are hard to deconvolute. This was not attempted in the original  $^2\text{H}$  NMR study since there was no reason to assume a population mix in the ground state of the protein. Only an orientational distribution caused by sample disorder (mosaic spread) had been included. Subsequent computer simulations of MAOSS spectra from the C18 ring methyl group, including minor components, did not yield another interpretation of the orientation in the major component in most cases but resulted in a small degree of uncertainty in the interpretation of the  $^2\text{H}$  NMR data.

The structural flexibility noted within the binding pocket (24–26) has mainly been associated with the location of the ring segment. In the most recent work (26), it was concluded that even various conformations locked within the chain segment are accommodated, not by relocating the chain, but by *cis* to *trans* ring flips being allowed within the protein. It was important to determine whether such ring flips could be induced in the chromophore by the processes of protein isolation and then reinsertion into saturated lipids, as used for the  $^2\text{H}$  NMR measurements. Work currently being undertaken in these and other (W. de Grip, Nijmegen) laboratories on rhodopsin regenerated with singly  $^{13}\text{C}$ -labeled retinals suggests that the conformation of the ring is not significantly perturbed when the protein is isolated and then introduced into the saturated phospholipid used in the  $^2\text{H}$  NMR measurements.

The only remaining major source of error in the previous structural determination from the  $^2\text{H}$  NMR measurements could come from some unreliability in other structural information used to combine the orientation information into a structural model, such as the degree and sense of twists along the length of the polyene chain of the chromophore (7). Indeed, some of these details remain contentious, as evidenced by recent efforts to confirm the sense of twist around the C12–C13 bond in the chain (27, 28). It is likely that such issues will only become fully settled with a complete high-resolution structure of the chromophore in rhodopsin.

#### ACKNOWLEDGMENT

We are grateful to W. de Grip (Nijmegen) for advice on rhodopsin regeneration, Martin Noble (Oxford) for generating the structural coordinates for 11-Z-retinal from the published crystal data, and Peter Fisher for technical assistance.

## REFERENCES

1. Mathies, R. A., and Lugtenburg, J. (2000) in *Handbook of Biological Physics* (Stavenga, D. G., de Grip, W. J., Pugh, E. N., Jr., Eds.) Vol. 3, p 55. Elsevier Science B. V., Amsterdam.
2. Feng, X., Verdegem, P. J. E., Lee, Y. K., Sandström, D., Edén, M., Bovee-Geurts, P., de Grip, W. J., Lugtenburg, J., de Groot, H. J. M., and Levitt, M. H. (1997) *J. Am. Chem. Soc.* **119**, 6853–6857.
3. Verdegem, P. J. E., Bovee-Geurts, P. H. M., de Grip, W. J., Lugtenburg, J., and de Groot, H. J. M. (1999) *Biochemistry* **38**, 11316–11324.
4. Smith, S. O., Palings, I., Miley, M. E., Courtin, J., de Groot, H., Lugtenburg, J., Mathies, R. A., and Griffin, R. G. (1990) *Biochemistry* **29**, 8158–8164.
5. Palczewski, K., Kumasaka, T., Hori, T., Behnke, C. A., Motoshima, H., Fox, B. A., Le Trong, I., Teller, D. C., Okada, T., Stenkamp, R. E., Yamamoto, M., and Miyano, M. (2000) *Science* **289**, 739–745.
6. Honig, B., Hudson, B., Sykes, B. D., and Karpus, M. (1971) *Proc. Natl. Acad. Sci. U.S.A.* **68**, 1289–1293.
7. Gröbner, G., Burnett, I. J., Glaubitz, C., Choi, G., Mason, A. J., and Watts, A. (2000) *Nature* **405**, 810–813.
8. Singh, D., Hudson, B. S., Middleton, C., and Birge, R. R. (2001) *Biochemistry* **140**, 4201–4204.
9. Creuzet, F., McDermott, A., Gebhard, R., van der Hoef, K., Spijker-Assink, M. B., Herzfeld, J., Lugtenburg, J., Levitt, M. H., and Griffin, R. G. (1991) *Science* **251**, 783–786.
10. Groesbeek, M., and Lugtenburg, J. (1992) *Photochem. Photobiol.* **56**, 903–908.
11. DeGrip, W. J., Daemen, F. J. M., and Bonting, S. L. (1980) *Methods Enzymol.* **67**, 301–320.
12. Verdegem, P. J. E. (1998) Ph.D. Thesis, University of Leiden.
13. DeLange, F., Bovee-Geurts, P. H. M., VanOostrum, J., Portier, M. D., Verdegem, P. J. E., Lugtenburg, J., and DeGrip, W. J. (1998) *Biochemistry* **37**, 1411–1420.
14. Raleigh, D. P., Levitt, M. H., and Griffin, R. G. (1990) *J. Chem. Phys.* **92**, 6347–6364.
15. Metz, G., Wu, X., and Smith, S. O. (1994) *J. Magn. Reson. A* **110**, 219–227.
16. Glaubitz, C. (1998) Ph.D. Thesis, University of Oxford.
17. Levitt, M. H., Raleigh, D. P., Creuzet, F., and Griffin, R. G. (1990) *J. Chem. Phys.* **92**, 6347–6364.
18. Herzfeld, J., and Berger, A. E. (1980) *J. Chem. Phys.* **73**, 6021–6030.
19. De Groot, H. J. M., Smith, S. O., Kolbert, A. C., Courtin, J. M. L., Winkel, C., Lugtenburg, J., Herzfeld, J., and Griffin, R. G. (1991) *J. Magn. Reson.* **91**, 30–38.
20. Abraham, R. J., and Loftus, P. (1978) *Proton and Carbon-13 NMR Spectroscopy*, p 33, Heyden & Son, London.
21. Kalinowski, H.-O., Berger, S., and Braun, S. (1988) *Carbon-13 NMR Spectroscopy*, p 118, John Wiley & Sons, Chichester.
22. Dalling, D. K., and Grant, D. M. (1972) *J. Am. Chem. Soc.* **94**, 5318–5324.
23. Gilardi, R. D., Karle, I. L., and Karle, J. (1972) *Acta Crystallogr. B* **28**, 2605–2612.
24. Nakanishi, K., Yudd, A. P., Crouch, R. K., Olson, G. L., Cheung, H.-C., Govindjee, R., Ebrey, T. G., and Patel, D. J. (1976) *J. Am. Chem. Soc.* **98**, 236–238.
25. Blatchly, R. A., Carriker, J. D., Balogh-Nair, V., and Nakanishi, K. (1980) *J. Am. Chem. Soc.* **102**, 2495–2497.
26. Jang, G.-F., Kuksa, V., Filipek, S., Bartl, F., Ritter, E., Gelb, M. H., Hoffmann, K. P., and Palczewski, K. (2001) *J. Biol. Chem.* **276**, 26148–26153.
27. Lou, J., Hashimoto, M., Berova, N., and Nakanishi, K. (1999) *Org. Lett.* **1**, 51–54.
28. Buss, V. (2001) *Chirality* **13**, 13–23.
29. Harbison, G. S., Smith, S. O., Pardo, J. A., Courtin, J. M. L., Lugtenburg, J., Herzfeld, J., Mathies, R. A., and Griffin, R. G. (1985) *Biochemistry* **24**, 6955–6962.
30. Harbison, G. S., Mulder, P. P. J., Pardo, H., Lugtenburg, J., Herzfeld, J., and Griffin, R. G. (1985) *J. Am. Chem. Soc.* **107**, 4809–4816.

BI020007O